EARTH SURFACE PROCESSES AND LANDFORMS
Earth Surf. Process. Landforms **43**, 124–133 (2018)

Published online 12 April 2017 in Wiley Online Library
(wileyonlinelibrary.com) DOI: 10.1002/esp.4149

Improving bank erosion modelling at catchment scale by incorporating temporal and spatial variability

Victoria Janes,[1,2] Ian Holman,[1]* Stephen Birkinshaw,[3] Greg O'Donnell[3] and Chris Kilsby[3]
[1] Cranfield Water Science Institute, Cranfield University, Bedford, UK
[2] Lancaster Environment Centre, Lancaster University, UK
[3] School of Civil Engineering and Geosciences, Newcastle University, Newcastle, UK

Received 14 September 2016; Revised 16 February 2017; Accepted 28 February 2017

*Correspondence to: Ian Holman, Cranfield Water Science Institute, Cranfield University, Bedford, MK43 0AL, UK. E-mail: i.holman@cranfield.ac.uk

ESPL
Earth Surface Processes and Landforms

ABSTRACT: Bank erosion can contribute a significant portion of the sediment budget within temperate catchments, yet few catchment scale models include an explicit representation of bank erosion processes. Furthermore, representation is often simplistic resulting in an inability to capture realistic spatial and temporal variability in simulated bank erosion. In this study, the sediment component of the catchment scale model SHETRAN is developed to incorporate key factors influencing the spatio-temporal rate of bank erosion, due to the effects of channel sinuosity and channel bank vegetation. The model is applied to the Eden catchment, north-west England, and validated using data derived from a GIS methodology. The developed model simulates magnitudes of total catchment annual bank erosion (617–4063 t y^{-1}) within the range of observed values (211–4426 t yr^{-1}). In addition, the model provides both greater inter-annual and spatial variability of bank eroded sediment generation when compared with the basic model, and indicates a potential 61% increase of bank eroded sediment as a result of temporal flood clustering. The approach developed within this study can be used within a number of distributed hydrologic models and has general applicability to temperate catchments, yet further development of model representation of bank erosion processes is required. © 2017 The Authors. Earth Surface Processes and Landforms published by John Wiley & Sons Ltd.

KEYWORDS: bank erosion; sediment; sinuosity; vegetation; catchment

Introduction

Sediment erosion and transport are natural geomorphic processes within river catchments, but high magnitude events and anthropogenic influences (such as deforestation and over-grazing) can easily disrupt the sensitive equilibrium between them. When these changes result in increased sediment loads, they may have numerous detrimental effects to the river system; increased sedimentation in channels and floodplains affecting land-use and changes in river morphology and behaviour (Owens *et al.,* 2005), flooding (Mcintyre *et al.,* 2012), and disruption to habitats and decreased biodiversity (e.g. salmonid spawning, Soulsby *et al.,* 2001). Furthermore, as sediments act as a transport vector for pollutants such as heavy metals, increased sediment delivery may also change the chemical composition of the river resulting in negative impacts to the ecosystem (eutrophication, Owens and Walling, 2002; and toxicity effects, Mackin *et al.,* 2003). Consequently, information on sediment generation and transport through river systems at a catchment scale, and their temporal and spatial variability is increasingly important to support catchment management.

Sediment fingerprinting techniques have been applied to a number of catchments worldwide to understand the relative importance of different sources of sediment, including eroded bank material. These suggest that bank erosion contributes significantly to catchment sediment budgets, in some cases representing up to 48% of total sediment supply (Walling, 2005; Walling *et al.,* 2008). Furthermore, where channel banks contain contaminated sediments the contribution of bank erosion to pollutant supply has also been noted to be significant; for example, lead supply from banks of 9 kg m^{-1} yr^{-1} (Glengonnar Water, Scotland UK, Rowan *et al.,* 1995) and mercury supply of 2.7 kg km^{-1} yr^{-1} (South River, Virginia USA, Rhoades *et al.,* 2009).

The severity of bank erosion is influenced by numerous factors such as the presence of bank vegetation (through both mechanical and hydrological factors) (Micheli and Kirchner, 2002; Simon and Collison, 2002; Bartley *et al.,* 2008); discharge and flow regime (Julian and Torres, 2006; Hooke, 2008; Surian and Mao, 2009); lithology (Hooke, 1980); channel confinement (Lewin and Brindle, 1977; Janes *et al.,* 2017); and anthropogenic influences (Winterbottom and Gilvear, 2000; Michalková *et al.,* 2011).

Rates of channel bank erosion are both highly temporally and spatially variable (Hooke, 1980; Bull, 1997; Lawler *et al.,* 1999; Couper *et al.,* 2002).

Management of sediment and other diffuse pollution issues at a catchment scale is imperative due to the connectivity of the system. Models provide a valuable means of estimating sediment generation and transport at catchment scales, potentially providing insights into the spatio-temporal generation and transport of sediment and the system responses to longer term changes such as climate change. However, many existing catchment-scale hydrological and water quality models contain no explicit representation of channel bank erosion processes; CREAMS - Chemicals, Runoff and Erosion from Agricultural Management Systems (Knisel, 1980), ANSWERS - Areal Nonpoint Source Watershed Environment Simulation (Beasley and Huggins, 1982), EPIC - Erosion Productivity Calculator (Sharpley and Williams, 1990), SWAT – Soil and Water Assessment Tool (Arnold *et al.,* 1998), and PSYCHIC – Phosphorus and Sediment Yield Characterisation In Catchments (Davison *et al.,* 2008). In addition, those models which do contain representations of bank erosion account for only a few of the numerous aforementioned factors controlling channel bank erosion rates which limits their ability to simulate the observed spatial and temporal variation of sediment generation through bank erosion processes. For example, the semi-distributed INCA-Sed model (Jarritt and Lawrence, 2007) accounts for bank eroded sediment within in-stream sediment sources using a power law relationship incorporating discharge and calibration parameters. As acknowledged by the authors, a range of sub-reach scale processes are not included within the model and therefore only a broad range of seasonal trends can be observed, rather than finer temporal and spatial variation. The model SedNet provides a mean-annual sediment budget (Prosser *et al.,* 2001; Wilkinson *et al.,* 2009). Riverbank erosion within the model is based on an empirical relationship related to stream power, the extent of channel bank vegetation, and non-erodible surfaces. While this method incorporates some factors influencing the spatial variation of bank erosion rates and provides an estimate of annual sediment generation, it does not account for finer-scale temporal variability or provide an indication of event-based bank erosion. While a dynamic version of the model (D-SedNet, Wilkinson *et al.,* 2014) exists, this model disaggregates longer term data to provide daily output, meaning the model is unable to fully capture the temporal variability observed in sediment loads.

Detailed numerical models of bank erosion have been shown to simulate channel migration with reasonable accuracy (Nagata *et al.,* 2000; Darby *et al.,* 2002, 2007; Duan, 2005). These models generally incorporate mathematical modelling of hydraulic bank properties, shear stresses acting on channel banks and subsequent erosion. However, these models lack simulation of catchment hydrology, and the high-resolution data required for such models and their computational requirements limit their application to reach scales. Therefore to provide estimates of bank-eroded sediment at a catchment scale, alternative methods are required.

If models are to provide the more holistic representation of sediment processes at a scale that is needed to inform catchment management, further research is needed to improve two key aspects of catchment models; continuous simulation of coupled hydrological and sediment processes, and the ability to replicate both temporal and spatial variability of natural systems. This paper, therefore, describes the further development and application of the Système Hydrologique Européen TRANsport (SHETRAN) model (Ewen *et al.,* 2000) to provide improved spatio-temporal representation of channel bank erosion processes within simulated catchment sediment budgets. The physically based model SHETRAN was chosen because of the ability of the model to represent both spatial and temporal variation of sediment generation through physical representation of these processes and their controlling factors. In particular, the paper shows how the modifications enable improved simulation of the temporal (through representation of bank vegetation removal and bank de-stabilisation associated with high magnitude events, and subsequent recovery) and spatial (by taking account of the influence of channel sinuosity) variation of bank eroded sediment generation within the Eden catchment in north-west England.

Methodology

SHETRAN (Systeme Hydrologique Europeen TRANsport) is a physically-based distributed model for catchment scale simulation of hydrology and transport (Ewen *et al.,* 2000). The model operates using a grid based representation of the catchment, with channel links situated along the edges of the grid cells. An option to include a more comprehensive representation of channel bank hydraulics can also be incorporated, resulting in an additional 10 m width grid cell between channel links and the adjacent grid cells. The temporal resolution of the model is typically 1 hour, although the timestep decreases during storm events to provide an improved representation of rapid infiltration and surface runoff processes. The processes represented within the hydrological and sediment components of the model are shown in Figure 1 and detailed within Birkinshaw *et al.,* 2014 and Elliott *et al.,* 2012. The following section details the development of the bank erosion component of SHETRAN and the application of the developed model is described in the subsequent section. Hereafter, the existing SHETRAN bank erosion model is termed

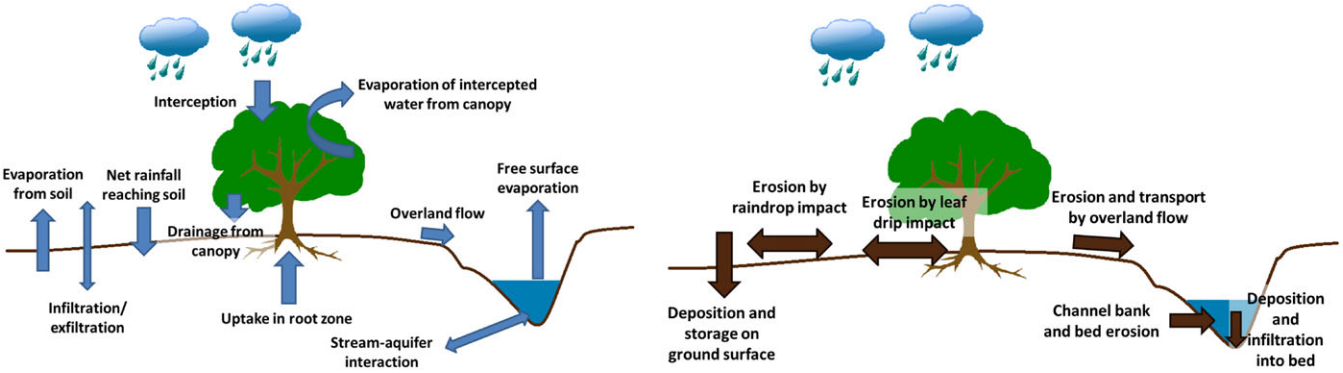

Figure 1. Hydrological and sediment erosion and deposition processes represented within the SHETRAN model. [Colour figure can be viewed at wileyonlinelibrary.com]

the 'basic' model and the revised model implemented within this study the 'enhanced' model.

Description of model improvements

The representation of bank erosion within the basic model is based on the exceedance of critical shear stress (τ_{bc}) acting on the channel banks. The critical shear stress is calculated using the Shield's curve method (similarly to Simon *et al.*, 2000). Bank erosion (E_b) is calculated as a rate of detachment of material per unit area of bank (kg m^{-2} s^{-1}) according to:

$$E_b = BKB.\left(\frac{\tau_b}{\tau_{bc}} - 1\right) \; where \tau_b > \tau_{bc} \tag{1}$$

where BKB is a bank erodibility parameter (kg m^{-2} s^{-1}), and τ_b is the shear stress acting on the channel bank (N m^{-2}) calculated as:

$$\tau_b = K\tau \tag{2}$$

where K is a proportionality constant calculated from channel width and flow depth and τ is the mean flow shear stress on the bed. While this equation accounts for the influence of varying discharge and, hence, shear stress acting on channel banks, all other significant factors (including those mentioned in the previous section) are not included. Therefore, the natural variation of bank erosion rates both spatially and temporally throughout catchments is likely to be underestimated.

Within the enhanced model, spatial variation of bank erosion is represented by way of the non-linear influence of local channel sinuosity on bank erosion. This is incorporated within the model by categorising channel sinuosity into one of three groups (similarly to channel curvature ratio categories as detailed by Crosato, 2009); channel links with low sinuosity (<1.2) have low erosion rates, moderately sinuous channels (1.2–1.5) have the highest erosion rates, and highly sinuous channels (>1.5) have erosion rates slightly lower than that of moderately sinuous channels (Janes, 2013).

Temporal variation of bank erosion as a result of the changing channel bank vegetation is represented within the model by varying the bank erodibility coefficient (BKB) between minimum and maximum values over time (see Figure 2). When channel discharge at a location in the catchment exceeds a threshold value (Q_{Thresh}) for that location the bank erodibility coefficient at that location increases to a maximum value (BKB_{max}). Q_{Thresh} represents the discharge at which vegetation within some parts of the reach is expected to be removed, and hence bank erodibility is increased. For outer-bends with little vegetation this increase in erodibility represents de-stabilisation of channel banks. Q_{Thresh} at the catchment outlet is set by the user (based on flood recurrence interval), and then each link is given a unique value of Q_{Thresh} calculated from the value of Q_{Thresh} at the outlet (the methodology used is detailed in the model application section). For all subsequent time steps of the model where the threshold value is not exceeded, the bank erodibility coefficient gradually decreases over time to the minimum value (BKB_{min}) at a rate set by the recovery factor (R):

$$BKB_t = BKB_{max} \; where \, Q \geq Q_{Thresh} \tag{3}$$

$$BKB_t = BKB_{t-1}.R \; where \, BKB_t > BKB_{min} \tag{4}$$

The difference in the magnitude of BKB_{min} and BKB_{max} represents the stabilising influence of vegetation on channel banks. The seasonal climate also influences the recovery factor (R), which reflects the potential rate of re-growth of bank vegetation and subsequent bank protection and stabilisation. R is calculated from the potential evapotranspiration (as a proxy for plant development) assuming that bank-side vegetation are not water-limited due to the shallow depth to the water table:

$$R = 1 - \left(k.\partial t.\left(\frac{PE_{obs}}{PE_{max}}\right)\right) \tag{5}$$

where PE_{max} represents the maximum daily potential evapotranspiration (mm s^{-1}), PE_{obs} (mm s^{-1}) is the observed potential evapotranspiration and ∂t is the length of the time-step (s). The parameter k controls the timescale of vegetation recovery and should reflect the type of vegetation in the catchment. Higher values of k, leading to quicker recovery times, are appropriate for species with the ability of rapid re-growth, such as willow (Salix fragilis). Table I shows the input parameters required for the developed bank erosion model.

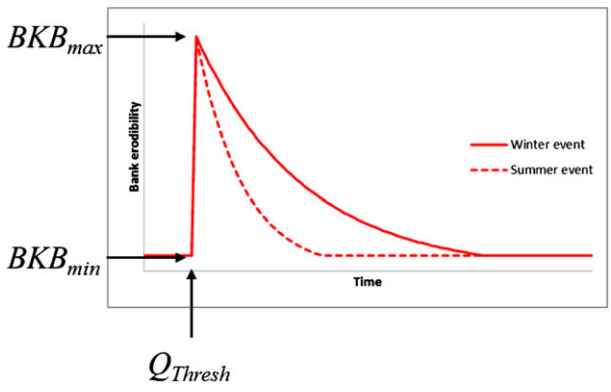

Figure 2. Schematic of temporal and seasonal variation of bank erodibility after an event where QThresh is exceeded. Time for erodibility to return to BKBmin after QThresh is exceeded is less in summer than in winter. [Colour figure can be viewed at wileyonlinelibrary.com]

Application of the enhanced model

The model was applied to the 2400 km^2 predominately rural Eden catchment in north west England, UK (see Figure 3). Topographical variation across the catchment (788 m AOD at the highest point, to 15 m at the outfall at the Sheepmount gauge) results in significant variation of average annual rainfall; the lower Eden receives approximately 800 mm yr^{-1} while upper reaches receive in excess of 2800 mm yr^{-1} (Mayes *et al.*, 2006).

The model was applied with a grid resolution of 1 km^2 (and bank cells with a length of 1 km and width of 10 m) with a maximum hourly temporal resolution. A 1 km^2 grid resolution reasonably captured the OS (Ordnance Survey – UK national mapping agency) channel network (shown by the blue line in Figure 3). The model was set up using a 30 m digital elevation model (Ordnance Survey, 2009), land-use (CEH, 2007), and soils (Wösten *et al.*, 1999). A daily 1 km^2 gridded daily rainfall product from 1990–2007 (Perry *et al.*, 2009) was used to specify the spatial rainfall, with tipping bucket rain gauge data then used to disaggregate the daily data to an hourly resolution

Table I. Model user input parameters required for the developed bank erosion model. Parameter Q_{Thresh} is scaled to the outlet value

Parameter	Units	Description
BKB_{min}	kg m^{-1} s^{-1}	Minimum bank erodibility
BKB_{max}	kg m^{-1} s^{-1}	Maximum bank erodibility
Q_{Thresh}	m^3 s^{-1}	Threshold discharge at which BKB for the link increases from BKBmin to BKBmax
K	N/A	Vegetation recovery speed (high values = rapid growing vegetation types)

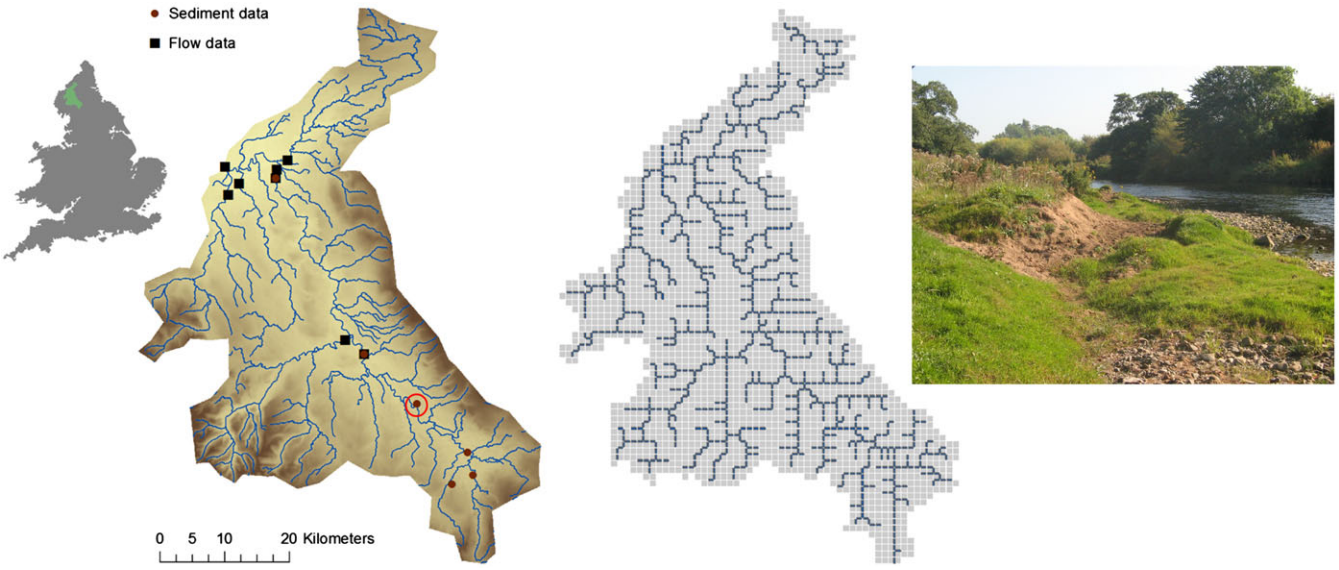

Figure 3. Eden catchment, Cumbria UK. Locations of gauging stations (black) and sediment data (brown) used for model calibration and validation are shown, and the model representation of the catchment and channel network. The photo inset shows a section of eroding bank near Kirkby Stephen (photo courtesy of Ken Rushton). [Colour figure can be viewed at wileyonlinelibrary.com]

to capture the shorter duration intensities. A simple nearest neighbour approach was applied to disaggregate the daily totals to hourly; for each grid cell, the shape of the nearest available hourly record was used to distribute the daily total to hourly intervals (see Lewis *et al.,* 2016 for further details).

The parameter Q_{Thresh}, which determines the discharge that leads to significant bank de-stabilisation and erosion, was derived in a three-stage process and has a unique value for each link scaled from the value of Q_{Thresh} at the outlet. First, the model was run using the long-term average daily rainfall (temporally constant, but spatially variable across the catchment) to derive steady-state simulated discharge at the catchment outlet, from which scaling factors were calculated for all links based on the ratio of local link flow to the outlet discharge. Second, the discharge magnitude at the catchment outlet for a flood of a return interval to represent Q_{Thresh} event was calculated using the annual maximum (AMAX) dataset (CEH, 2015) covering 46 hydrological years (1966–2012), the median of annual maximum values (Q_{med}) and a Generalised Logistic growth curve (estimated using L-moments, see Flood Estimation Handbook, Faulkner, 1999). For a given return period T:

$$Q_T = x_T . Q_{MED} \tag{6}$$

where Q_T is the discharge for an event with return interval (T), x_T is the growth factor (the value of the growth curve at a given return period). Finally, the corresponding Q_{Thresh} values throughout the catchment were calculated by multiplying Q_{Thresh} value at the catchment outlet by the scaling factors.

All channel links within SHETRAN representations are located between two channel bank cells and have a default sinuosity of 1. Therefore a GIS-based channel network was used to estimate sinuosity for each link. Sinuosity was measured across the catchment using WFD river waterbodies data (Environment Agency, 2012) and GIS; a channel network polyline was split into reaches of equal length, and sinuosity calculation for each reach was calculated as the channel distance divided by the straight-line distance between reach start and end points. As the value of sinuosity is dependent on the reach length at which it is measured, this process was repeated for a range of length scales. The length scale with the largest peak in variance of sinuosity (measurement length of 975 m) was used as this best captured the variation of sinuosity across the catchment.

Model calibration and validation

After a 1 year 'start-up' period in which groundwater levels tended to an equilibrium, the model was run from 1991–2001 for parameter calibration, and 2001–2007 for validation. Similarly to previous studies using SHETRAN (Lukey *et al.,* 2000; Bathurst *et al.,* 2006; Elliott *et al.,* 2012) calibration parameters included the overland and channel flow resistance coefficients, with calibration conducted manually due to the computational requirements of the model. The hydrological component of the model was compared with hourly and daily hydrological data from the National River Flow Archive (CEH, 2015) gauging stations and HiFlows data sets (see Figure 3). From this a range of parameter value sets were derived (see Table II) based on parameters to which the simulated flows were most sensitive (Lukey *et al.,* 2000; Bathurst *et al.,* 2006). The

Table II. Validated parameter values for the Eden catchment model

Parameter/function	Low value	High value
Hydrological		
Strickler overland flow resistance coefficient	1	3
Saturated hydraulic conductivity in channel soil (mm day^{-1})	0.1	60
Channel bank Strickler coefficients (x and y directions)	20	30
Sediment		
Overland flow erodibility (kg m^{-2} s^{-1})	0.02	0.05
Raindrop impact erodibility (J^{-1})	2E-12	1E-11

simulation outputs were then superimposed on each other, providing an envelope of minimum and maximum model estimates of river flows.

Analysis of peak-over-threshold (POT) events was also conducted as part of the validation process to ensure the model could accurately reproduce high-magnitude events, using POT data from the NRFA (CEH, 2015). For each POT event the observed event maximum discharge was compared with the maximum simulated discharge within 24 h either side of the event timing. The average percentage error of simulated POT events was then calculated within the calibration/validation periods for each gauging station.

The bank erodibility parameters (see Table III) were calibrated by comparison with observed bank erosion values derived using an historical map overlay methodology in GIS, further details of which can be found in Janes *et al.* (2017). Channel banklines were digitised for the Eden and main tributaries Caldew, Irthing, Lyvennet, Eamont and Petteril from Historical OS maps for the five available years (1880, 1901, 1956, 1970, and 2012) with consecutive banklines overlaid to provide an area of bank erosion. As smaller tributaries are often represented on OS maps as a single line (particularly on older maps) it is not possible to calculate bank erosion values for these channels using this methodology. To account for potential geo-referencing and mapping errors within the data, the eroded area was calculated using the simple overlay procedure, and also applying a buffer of 3.5 m to the older channel, providing upper and lower erosion estimates respectively. Minimum and maximum bank height estimates were calculated from the two bank heights provided within the RHS survey data, to account for error within the estimate. Minimum and maximum estimates of annual bank eroded sediment were estimated for each sub-catchment using this procedure. While alternative methods of data collection such as erosion pin methodologies can provide estimates of bank eroded sediment at a finer temporal resolution (event scale), these methods are limited spatially and cannot provide catchment wide estimates of bank erosion and are therefore unsuitable for this study.

Table III. Calibrated parameter values of the bank erosion model

	Parameter		Calibrated value
	Return period of Q_{Thresh}		12
	k		0.03
	Factoral difference between BKB_{min} and BKB_{max}		20
	Straight channels	**Meandering channels**	**Highly sinuous channels**
Sinuosity	**<1.2**	**1.2–1.5**	**>1.5**
BKB_{min}	3.5E-11	9.6E-11	7.0E-11
BKB_{max}	7.0E-10	1.9E-09	1.4E-09

Preliminary magnitudes of differences in erosion rates between vegetated and non-vegetated banks, and parameters influencing the length of recovery time were based on literature of riparian growth rates of vegetation types found in the area (Environment Agency, 1998). The recovery factor was calibrated as 3 months during summer according to bank vegetation growth rates in Environment Agency, 1998. The return period of an event used to calibrate the Q_{Thresh} parameter was guided by literature evidence and was based on an event with return period of greater than 12 years. The variation of bank erodibility with channel sinuosity was parameterized based on Janes (2013); bank erosion rates at channel sinuosities around the threshold value of sinuosity (~1.5) are approximately 2.75 times greater than straight channels (low sinuosities), and in highly sinuous channels (>1.5) approximately 2 times greater.

Model simulations with the sediment component were conducted across the range of hydrological parameters specified in Table II, so that the simulated suspended sediment load and bank erosion values incorporate the effects of the hydrological parameter uncertainty. Similarly to the hydrological component of the model, minimum and maximum parameter values were set for sensitive sediment parameters, and simulations were conducted using a range of parameter values within this range (see Table II). Simulated annual sediment loads were calculated and compared with those predicted by sediment rating curves, derived using grab samples and turbidity data collected from several locations between November 2006 and March 2009 (see Figure 4) by the CHASM (Catchment Hydrology And Sustainable Management) project (Mills, 2009). These were then used in conjunction with either gauging station data or simulated discharge to provide estimates of annual sediment loads at these locations.

The sensitivity of the enhanced model to temporal flood clustering was analysed with respect to the magnitude of bank eroded sediment. To do this the model was run with a 1 year start-up period, and then 3 days of rainfall (taken from the January 2005 event, 6/01/2005–8/01/2005 inclusive with a peak discharge at Sheepmount of 1516.3 m^3 s^{-1}, as this was a notable high magnitude event). A temporally constant rainfall was then used for 1 week before a second smaller rainfall event that did not exceed Q_{Thresh}. The model was then re-run with 2, 4, 6, 8 and 12 week gaps between the two events. Constant temporal rainfall input between the two events was used to ensure identical antecedent hydrological conditions prior to the second event so that simulated differences in the magnitude of bank eroded sediment were due solely to event timing.

Results

Hydrological assessment

Table IV shows the average hourly hydrological performance statistics of the model for the validation period (and daily statistics at Kirkby Stephen where hourly flow data were unavailable). All hourly NSE and R^2 values are above 0.55 and 0.7, respectively, indicating satisfactory model performance at all sites (Moriasi *et al.,* 2007). The simulated absolute percentage bias is below 25% at all gauging stations (indicating satisfactory model performance according to Moriasi *et al.,* 2007) and at five of the eight stations is less than 8%.

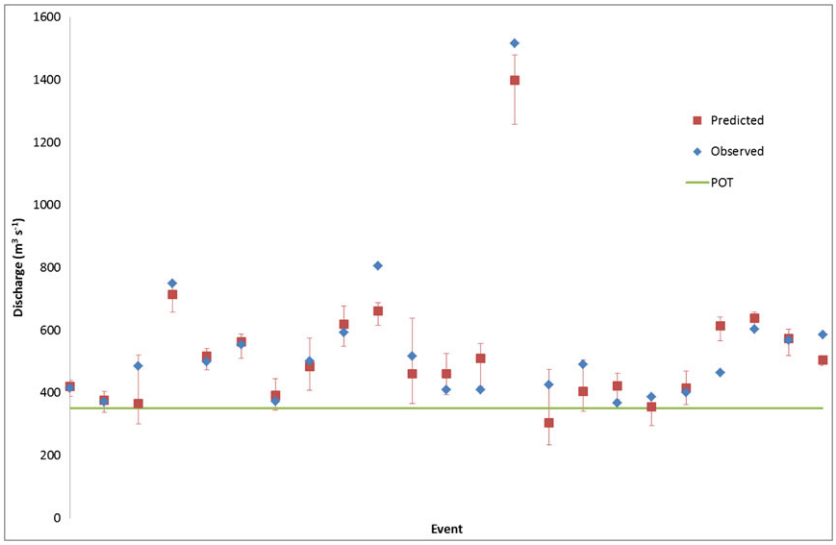

Figure 4. Simulated and observed peak over threshold events at Sheepmount gauging station during the model validation period (1/1/2001–1/1/2007). [Colour figure can be viewed at wileyonlinelibrary.com]

Table IV. Average performance statistics from the simulation of hourly flows across the Eden catchment (with the exception of Kirkby Stephen based on daily flows) during the validation period

Catchment/sub-catchment	Gauging station	Upstream area (km^2)	NSE	R^2	PBIAS (%)
	Sheepmount	2286	0.901	0.911	3
	Great Corby	1373	0.857	0.869	3
	Temple Sowerby	616	0.857	0.873	8
Eden	Kirkby Stephen*	69	0.848	0.878	14
Irthing	Greenholme	334	0.726	0.809	20
Petterill	Harraby Green	160	0.630	0.796	–16
Caldew	Cummersdale	244	0.830	0.835	8
Eamont	Udford	396	0.598	0.713	–3

Table V. Percentage of peak over threshold events within the simulated range during the validation period, and average percentage error of simulated peak discharge

Channel	Location	Percentage of simulated events within 15% of the observed event	Average error of event discharge simulation (%)
	Sheepmount	91	–1
	Great Corby	88	–1
	Temple Sowerby	47	–19
Eden	Kirkby Stephen	22	–44
Irthing	Greenholme	8	–51
Petterill	Harraby Green	38	19
Caldew	Cummersdale	31	–37
Eamont	Udford	60	28

The POT analysis indicates the model's ability to predict high-magnitude events (see Figure 4 and Table V). Although the model under-estimates event peak flow at most locations, as is common with other hydrological models (Van Liew *et al.,* 2003; Butts *et al.,* 2004), 65% of POT events were within the simulated uncertainty range at the catchment outlet at Sheepmount (Table IV and Figure 4). It should be noted that the gauging station on the Irthing at Greenholme is often affected by backwater from the Eden at medium–high flows, which could partially explain the lower peak over threshold simulation accuracy observed at this location (Table V).

Bank erosion

The GIS overlay methodology indicates the total mass of sediment generated through bank erosion processes within the catchment is between 539 and 2346 t yr^{-1} (Table VI). The estimates from both GIS methodologies provide an uncertainty range between 211 and 4426 t yr^{-1}. Total annual simulated bank erosion in Table VII is higher than the most recent observed average annual bank erosion rates (1970–2012 – Table VI) but within the observed uncertainty range over the historical. In addition, Table VII indicates that the enhanced model simulates a greater inter-annual variability of average annual bank erosion rates than the basic model. The enhanced model also simulates a greater range of spatial variation of bank erosion throughout the catchment than the basic model. The

Table VI. Observed bank erosion rates (t yr^{-1}) from each overlay time period. Values shown are averages from all methodological estimates

Channel	1880–1901	1901–1956	1956–1970	1970–2012
Eden	1329	682	1612	198
Petteril	136	58	209	29
Caldew	412	187	439	117
Irthing	356	216	487	166
Lyvenet	55	26	59	12
Eamont	58	17	44	16
Total	**2346**	**1186**	**2849**	**539**

Table VII. Annual bank erosion for the whole catchment as simulated by both the basic and enhanced models during the validation period. Values are in t yr^{-1}

		2001	2002	2003	2004	2005	2006
	Minimum	721	1655	617	1686	2842	622
	Maximum	4063	2833	2219	2682	3898	2784
Enhanced	Average	2331	2120	1401	2093	3350	1400
	Minimum	1951	3170	1542	2907	2356	2943
	Maximum	2126	3355	1728	3129	2539	3183
Basic	Average	2001	3234	1588	2972	2404	3013

basic version of the model was parameterised so that the total catchment average annual mass of bank eroded sediment generation was similar to the enhanced model to enable comparison of spatial bank erosion simulation in Figure 5. The observed data used for comparison here is taken from the upper estimate. The basic version of the model (Figure 5(A)) simulates a fairly spatially constant magnitude of bank erosion throughout the catchment in comparison wih the enhanced model (Figure 5(B)) and the observed data (Figure 5(C)). The model was also validated at a sub-catchment scale using Water Framework Directive sub-catchment boundaries by correlating the total simulated bank eroded sediment of the basic and enhanced versions of the model with the observed data. Correlations between simulated and observed data indicate that the enhanced model provides a more accurate spatial estimation of bank erosion at the sub-catchment level (R=0.500, *P*=0.007) compared with the basic model (R=0.367, *P*=0.048). These correlation values indicate an improvement in the spatial variability of bank erosion simulated by the developed model, but nevertheless the overall predictive ability of the spatial variability is poor for reasons detailed within the discussion.

Sediment load accuracy

Table VIII shows observed annual sediment loads with upper and lower 95% confidence intervals (calculated from the coefficient of the rating curve equations from Mills, 2009), and simulated annual sediment loads with upper and lower bounds based on the parameter set used for simulation. The confidence intervals of the observed sediment loads incorporate both hydrological and sediment parameterisation uncertainty and are of a similar magnitude to the uncertainty bounds of simulated sediment loads. Furthermore, the ranges of simulated and observed sediment loads overlap at all locations.

Sensitivity to temporal flood clustering

Values of bank eroded sediment generation for each of the five temporal flood cluster scenarios was calculated by summing the total catchment bank erosion for 31 days, starting from the date of the second rainfall event (see Table IX). The model indicates bank eroded sediment generated from a single flood event may be up to 61% greater if the event occurs within 2 weeks of a large flood event. As the temporal separation of the two flood events increases the magnitude of bank erosion caused by the second event decreases. Once channel bank vegetation has recovered from the first event, subsequent events below the threshold discharge do not result in increased magnitudes of bank erosion.

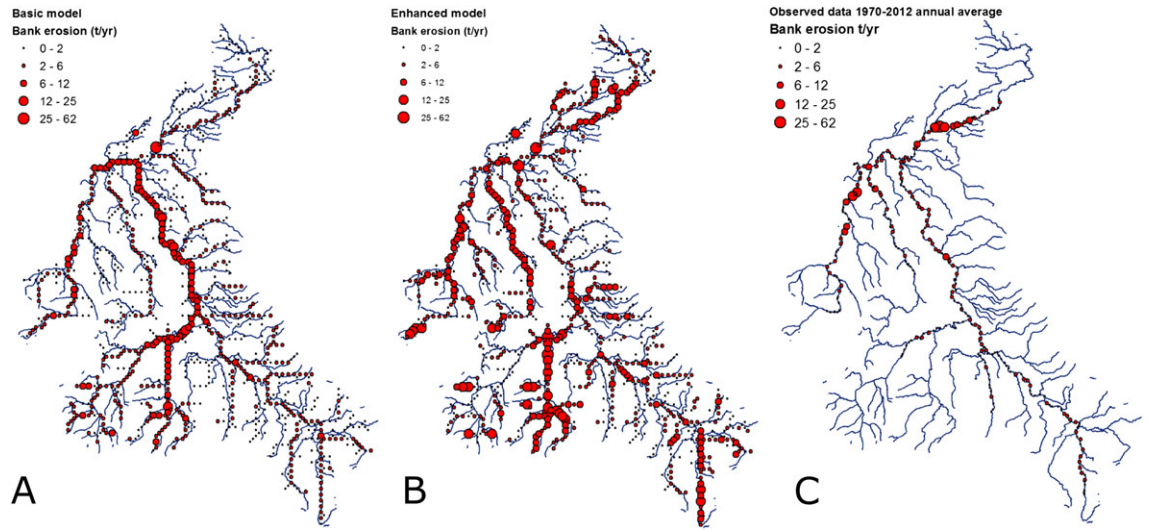

Figure 5. Average annual bank erosion (A) simulated by the basic model, (B) simulated by the enhanced model, (C) observed from GIS data. Small tributaries are not included within the observed data as discussed in the methodology. [Colour figure can be viewed at wileyonlinelibrary.com]

Table VIII. Observed and simulated average annual sediment loads (t yr^{-1})

Location	Observed average	Simulated average	Observed 95% confidence range	Simulated range
Great Corby	21968	21254	10325–43277	11366–31956
Temple Sowerby	16016	9121	6086–26106	4871–13654
Appleby	15364	5827	1229-16747	3116–8774
Great Musgrave	5126	4263	1794–7945	2197–6479
Kirkby Stephen	1794	1528	736–3086	758–2362
Smardale	444	739	164–719	368–1147

Table IX. Model sensitivity to temporal sequencing of flood events. Bank erosion values shown are summed from the whole catchment over a period of 31 days, starting from the beginning of the second rainfall event

Time between flood events (weeks)	Monthly bank erosion during second event (t)
1	851
2	681
4	547
6	536
8	530
12	528

Discussion

Observed bank erosion rates within this study determine the significance of channel bank erosion as a sediment source within the Eden catchment, Cumbria. Based on average annual simulated sediment load at Sheepmount, the data collected indicate that bank erosion represents 5–11% of the annual catchment sediment budget. This value is at the lower end of the range observed within other UK catchments (Walling, 2005; Walling *et al.,* 2006; Bartley *et al.,* 2007) which could be partly due to the predominance of grassland within the catchment.

The GIS dataset also indicates significant temporal variability of average annual bank erosion rates between the four time periods analysed, but does not fully capture the inter-annual variability. Several previous studies have noted significant inter-annual variability of bank erosion processes (Hooke, 2008; Kronvang *et al.,* 2013). Simulated bank eroded sediment generation using the enhanced model shows greater inter-annual variation of bank erosion rates than those of the basic model (Table VII), with the highest values during the year 2005. This is expected as the largest event discharge recorded during the study period (and second largest to date) at this station occurred during the January of this year (8/1/2005 1516.3 m^3 s^{-1}). Previous studies have indicated the significance of high magnitude events to bank erosion (Hooke, 1979; Julian and Torres, 2006; Henshaw *et al.,* 2012; Palmer *et al.,* 2014). The developed representation of bank erosion processes enables model sensitivity to high magnitude events, and therefore replication of observed temporal (inter-annual) variability of sediment generation.

The observed average annual bank erosion rates for the years 1970–2012 shown in Table VI are lower than average simulated values for 2001–2006. The observed data present an average annual bank erosion value across several years and inter-annual variation within time periods, as a result of flood rich and poor years, is not represented. The average annual maximum discharge recorded at Sheepmount from 1970–2012 was considerably lower than between 2001 and 2006 (647m^3 s^{-1} and 764m^3 s^{-1}, respectively). Therefore bank erosion rates between 2001 and 2006 would be expected to be higher than the 1970–2012 average. Furthermore, observed data show total bank erosion within six main channels of the Eden catchment, additional smaller tributaries have not been included, yet simulated values include the whole catchment as represented by the model. The lower estimates of observed bank erosion are taken from the GIS overlay methodology with a 3.5 m buffer applied to account for errors within the mapping process, which for more recent maps (such as 1970 and 2012) should be less significant than for earlier maps. Therefore the lower estimate of actual bank erosion for the 1970–2012 time period is potentially a significant underestimate of reality.

The enhanced model simulates sensitivity to flood clustering, by incorporating an element of catchment recovery following a large event. The results indicate that bank eroded sediment generation for an event of the same magnitude may vary depending on the event timing. Previous studies have noted the importance of antecedent conditions to bank erosion processes; Hooke (1979) noted that while event-based bank erosion at certain sites was correlated with discharge of the previous peak, the influence of this variable is complex. Previous high flows can weaken banks by undercutting but can also remove loose bank material leaving the bank more resistant to subsequent high flows. Thorne (1982) observed that mass failure of banks can result in an increase in bank stability due to supply of sediment to the basal zone, unless critical shear stress for removal of this basal material is exceeded. The enhanced model developed in this study provides an additional element of catchment memory for bank erosion and enables simulation of the effects of event clustering, and influence of antecedent conditions. The frequency of high magnitude events within the UK is expected to increase with projected climatic changes (Bell *et al.,* 2012; Kay *et al.,* 2014; Madsen *et al.,* 2014). Therefore, to enable climate-proof catchment management practices models will be required to represent the effects of flood clustering.

The spatial variation of bank erosion simulated by the basic model was controlled solely by flow variation (and hence variation of shear stress) throughout the catchment. As shown in Figure 5(A) this resulted in little variation of simulated bank erosion across the catchment. Significant spatial variation was observed from the GIS analysis within this study (Figure 5(C)), and has been observed within several additional UK catchments (Bull, 1997; Lawler *et al.,* 1999). The inclusion of sinuosity within the enhanced model enables simulation of some spatial variability of bank erosion rates within the catchment (Figure 5(B)). Correlation of sub-catchment totalled bank erosion rates indicate that bank erosion predicted by the enhanced model is more accurate than the basic model, yet still provides a weak fit of the observed bank erosion rates throughout the catchment. Several factors such as anthropogenic influences, lithology, channel confinement, bank height, and slope influence bank erosion rates resulting in the significant observed spatial variability within catchments. While sinuosity is known to be one factor influencing the spatial variation of bank erosion (Micheli and Kirchner, 2002; Janes, 2013) many of these additional factors are not included within the developed model due to current limited understanding of their behaviour, complex interactions, and lack of spatial data coverage. Therefore some differences between the simulated and observed bank erosion rates are to be expected due to the omission of many of these factors and the widely recognised difficulty of capturing the naturally high variability in bank erosion rates. Comparisons of observed and model simulated bank erosion values such as those in Figure 5 are rarely performed but these types of analyses are required if models are to be judged useful in management at the local scale. The model can be used to assist identification of areas where bank erosion would be expected to occur naturally, and comparison with observational data can indicate areas where bank erosion is prevented/accelerated due to anthropogenic factors not included within the model.

The observed bank erosion data within this study provides an estimate of annual bank eroded sediment generation with greater spatial resolution and over a longer timescale than is possible using field-based techniques (such as erosion pins). However, it is not possible to accurately estimate event-based bank eroded sediment using data derived from this methodology. Further data (such as LIDAR analysis of bank migration at a finer temporal

scale) and analysis is required to calibrate the model and assess performance during individual events.

Conclusions

Channel bank erosion contributes a significant proportion of catchment sediment budgets and yet is commonly excluded or overly simplified within catchment scale models. In this study, the bank erosion component within the physically-based SHETRAN model has been further developed to incorporate both temporal and spatial variability of bank erosion by inclusion of additional controlling factors; removal of bank vegetation and bank collapse after a flood event and subsequent recovery, and channel sinuosity. The developments within this study improve the representation of natural processes influencing bank erosion rates, and enable representation of catchment sensitivity to flood event clustering.

The model has been successfully applied to the Eden catchment, north-west England, and validated using hydrological, bank erosion and suspended sediment data. The enhanced model has been shown to simulate improved inter-annual and spatial variability of catchment scale bank eroded sediment generation when compared with the basic model, yet it is noted that the developed model still provides a weak fit with observed data. Differences between the spatial variation of observed and simulated bank erosion rates are attributed to additional factors not included within the model due to limitations in current understanding and data availability. Simulated sediment loads were compared with observational data, and while uncertainty in both observed and predicted sediment loads is large, values were found to overlap throughout the catchment, indicating reasonable accuracy of model simulations. While the accuracy of spatial bank erosion simulations is currently insufficient to support application of the model for management purposes the study represents a contribution to the research need for continuing development of sediment models. The developed representation of bank erosion processes that have been applied to the SHETRAN model in this study could also be applied to a number of existing physically based models.

The developed representation of sediment source estimation within the model provides a more holistic representation of sediment processes throughout the catchment. The resultant model provides an improved representation of the spatial and temporal variability of sediment loads, yet further development of such models is required to provide estimates of sediment loads with sufficient accuracy to support management of diffuse pollution.

Acknowledgements—We would like to thank the two anonymous reviewers for their helpful and constructive comments that assisted in improving this manuscript. This work was funded by EPSRC as part of the FloodMEMORY project EP/K013513/1. Additional thanks go to the Environment Agency for the provision of channel survey and bank height data, Cranfield University for LandIS soil data, and the CHASM project and Carolyn Mills for sediment data. The associated metadata/data presented in this research can be accessed using the following DOIs: 10.17862/cranfield.rd.4300220, 10.17862/cranfield.rd.4300202.

References

Arnold JG, Srinivasan R, Muttiah RS, Williams JR. 1998. Large-area hydrologic modelling and assessment: Part 1. Model development. *JAWRA Journal of the American Water Resources Association* **34**: 73–89.

Bartley R, Hawdon A, Post DA, Roth CH. 2007. A sediment budget for a grazed semi-arid catchment in the Burdekin basin, Australia. *Geomorphology* **87**: 302–321.

Bartley R, Keen RJ, Hawdon AA, Hairsine PB, Disher MG, Kinset-Henderson AE. 2008. Bank erosion and channel width change in a tropical environment. *Earth Surface Processes and Landforms* **33**(14): 2147–2200.

Bathurst JC, Burton A, Clarke BG, Gallart F. 2006. Application of the SHETRAN basin-scale, landslide sediment yield model to the Llobregat basin, Spanish Pyrenees. *Hydrological Processes* **20**: 3119–3138.

Beasley DB, Huggins LF. 1982. ANSWERS – Users manual. In *EPA-905/9-82-001, USEPA, Region 5*. IL: Chicago.

Bell VA, Kay AL, Cole SJ, Jones RG, Moore RJ, Reynard NS. 2012. How might climate change affect river flows across the Thames Basin? An area-wide analysis using the UKCP09 Regional Climate Model ensemble. *Journal of Hydrology* **442–443**: 89–104.

Birkinshaw SJ, Bathurst JC, Robinson M. 2014. 45 years of non-stationary hydrology over a forest plantation growth cycle, Coalburn catchment, Northern England. *Journal of Hydrology* **519**: 559–573.

Bull LJ. 1997. Magnitude and variation in the contribution of bank erosion to the suspended sediment load of the River Severn, UK. *Earth Surface Processes and Landforms* **22**: 1109–1123.

Butts MB, Payne JT, Kristensen M, Madsen H. 2004. An evaluation of the impact of model structure on hydrological modelling uncertainty for streamflow simulation. *Journal of Hydrology* **298**: 242–266.

Centre for Ecology and Hydrology (CEH). 2007. Land Cover Map http://www.ceh.ac.uk/services/land-cover-map-2007 (accessed on 27/8/2015).

Centre for Ecology and Hydrology (CEH). 2015. National River Flow Archive http://nrfa.ceh.ac.uk/ (accessed on 27/8/2015)

Couper P, Stott TIM, Maddock IAN. 2002. Insights into river bank erosion processes derived from analysis of negative erosion-pin recordings: observations from three recent UK studies. *Earth Surface Processes and Landforms* **79**: 59–79.

Crosato A. 2009. Physical explanations of variations in river meander migration rates from model comparison. *Earth Surface Processes and Landforms* **34**: 2078–2086.

Darby SE, Alabyan AM, Van de Wiel MJ. 2002. Numerical simulation of bank erosion and channel migration in meandering rivers. *Water Resources Research* **38**: 1163.

Darby SE, Rinaldi M, Dapporto S. 2007. Coupled simulations of fluvial erosion and mass wasting for cohesive river banks. *Journal of Geophysical Research* **112**: F03022.

Davison PS, Withers PJ, Lord EI, Betson MJ, Strömqvist J. 2008. PSYCHIC – a process-based model of phosphorus and sediment mobilisation and delivery within agricultural catchments. Part 1: Model description and parameterisation. *Journal of Hydrology* **350**: 290–302.

Duan JG. 2005. Analytical approach to calculate rate of bank erosion. *Journal of Hydraulic Engineering* **131**: 980–990.

Elliott AH, Oehler F, Schmidt J, Ekanayake JC. 2012. Sediment modelling with fine temporal and spatial resolution for a hilly catchment. *Hydrological Processes* **26**: 3645–3660.

Environment Agency. 1998. Revetment Techniques Used on the River Skerne Restoration Project. Technical Report W83.

Environment Agency. 2012 WFD River Waterbodies data. https://data.gov.uk/dataset/wfd-river-waterbodies Accessed 9/7/2015.

Ewen J, Parkin G, O'Connell PE. 2000. SHETRAN: distributed river basin flow and transport modeling system. *Journal of Hydrologic Engineering* **5**: 250–258.

Faulkner D. 1999. *Flood Estimation Handbook*, Vol. **2: Rainfall Frequency Estimation**. Institute of Hydrology: Wallingford UK.

Henshaw AJ, Thorne CR, Clifford NJ. 2012. Identifying causes and controls of river bank erosion in a British upland catchment. *Catena* **100**: 107–119.

Hickin E. 1978. Mean flow structure in meanders of the Squamish River, British Columbia. *Canadian Journal of Earth Sciences* **15**: 1833–1849.

Hooke J. 1979. An analysis of the processes of river bank erosion. *Journal of Hydrology* **42**: 39–62.

Hooke J. 1980. Magnitude and distribution of rate of river bank erosion. *Earth Surface Processes* **5**: 143–157.

Hooke JM. 2008. Temporal variations in fluvial processes on an active meandering river over a 20-year period. *Geomorphology* **100**: 3–13.

Janes VJ. 2013. An analysis of bank erosion and development of a catchment sediment budget mode. Unpublished PhD thesis, University of Exeter.

Janes VJ, Nicholas AP, Collins A, Quine T. 2017. Analysis of fundamental physical factors influencing channel bank erosion: results for contrasting catchments in England and Wales. *Environmental Earth Sciences* in press. https://doi.org/10.1007/s12665-017-6593-x.

Jarritt N, Lawrence D. 2007. Fine sediment delivery and transfer in lowland catchments: modelling suspended sediment concentrations in response to hydrological forcing. *Hydrological Processes* **2744**: 2729–2744.

Julian J, Torres R. 2006. Hydraulic erosion of cohesive riverbanks. *Geomorphology* **76**: 193–206.

Kay AL, Crooks SA, Davies HN, Prudhomme C, Reynard NS. 2014. Probabilistic impacts of climate change on flood frequency using response surfaces 1: England and Wales. *Regional Environmental Change* **14**: 1215–1227.

Knisel W. 1980. CREAMS A field scale model for Chemicals Runoff and Erosion from Agricultural Management Systems. USDA Conservation Research Report.

Kronvang B, Andersen HE, Larsen SE. 2013. Importance of bank erosion for sediment input, storage and export at the catchment scale. *Journal of Soils and Sediments* **13**: 230–241.

Lawler DM, Grove JR, Couperthwaite JS, Leeks GJL. 1999. Downstream change in river bank erosion rates in the Swale - Ouse system, northern England. *Hydrological Processes* **13**: 977–992.

Lewin G, Brindle B. 1977. Confined meanders. In *River Channel Changes*, Gregory K (ed). Wiley: Chichester; 221–233.

Lewis E, Birkinshaw S, Quinn N, Freer J, Coxon G, Woods R, Bates P, Fowler H. 2016. A gridded hourly rainfall dataset for the UK applied to a national physically-based modelling system. *Geophysical Research Abstracts* **18**: 14348.

Lukey BT, Sheffield J, Bathurst JC, Hiley RA, Mathys N. 2000. Test of the SHETRAN technology for modeling the impact of restoration on badlands runoff and sediment yield at Draix, France. *Journal of Hydrology* **235**: 44–62.

Mackin MG, Brewer PA, Balteamu D, Coulthard TJ, Driga B, Howard AJ, Zaharia S. 2003. The long term fate and environmental significance of contaminant metals released by the January and March 2000 mining tailings dam failures in Maramureş County, upper Tisa Basin, Romania. *Applied Geochemistry* **18**: 241–257.

Madsen H, Lawrence D, Lang M, Martinkova M, Kjeldsen TR. 2014. Review of trend analysis and climate change projections of extreme precipitation and floods in Europe. *Journal of Hydrology* **519**: 3634–3650.

Mayes WM, Walsh CL, Bathurst JC, Kilsby CG, Quinn PF, Wilkinson ME, Daugherty AJ, O'Connell PE. 2006. Monitoring a flood event in a densely instrumented catchment, the Upper Eden, Cumbria, UK. *Water and Environment Journal* **20**: 217–226. https://doi.org/10.1111/j.1747-6593.2005.00006.x.

Mcintyre N, Ballard C, Bulygina N, Frogbrook Z, Cluckie I, Dangerfield S, Ewen J, Geris J, Henshaw A, Jackson B, Marshall M, Pagella T, Park JS, Reynolds B, O'Connel E, O'Donnell G, Sinclar F, Solloway I, Thorne C, Wheater H. 2012. *The potential for reducing flood risk through changes to rural land management: outcomes from the Flood Risk Management Research Consortium*. BHS Eleventh National Symposium: Dundee.

Michalková M, Piégay H, Kondolf GM, Greco SE. 2011. Lateral erosion of the Sacramento River, California (1942–1999), and responses of channel and floodplain lake to human influences. *Earth Surface Processes and Landforms* **36**: 257–272.

Micheli E, Kirchner J. 2002. Effects of wet meadow riparian vegetation on streambank erosion. 1. Remote sensing measurements of streambank migration and erodibility. *Earth Surface Processes and Landforms* **27**: 627–639.

Mills C. 2009. Spatial variability and scale dependency of sediment yield in a rural river system – the river Eden, Cumbria, UK. Newcastle University, UK. Unpublished PhD thesis.

Moriasi DN, Arnold JG, VanLie MW, Bingner RL, Harmel RD, Veith TL. 2007. Model evaluation guidelines for systematic quantification of accuracy in watershed simulations. *Transactions of the ASABE* **50**: 885–900.

Nagata N, Hosoda T, Muramoto Y. 2000. Numerical analysis of river channel processes with bank erosion. *Journal of Hydraulic Engineering* **126**: 243–252.

Ordnance Survey. 2009. OS land-form PANORAMA DTM, 1:50000. Digimap: EDINA supplied service, available at: htt[://digimap.edina.ac.uk/

Owens PN, Batalla RJ, Collins AJ, Gomez B, Hicks DM, Horowitz AJ, Kondolf GM, Marden M, Page MJ, Peacock DH, Pettocrew EL, Salomons W, Trustrum NA. 2005. Fine-grained sediment in river systems: environmental significance and management issues. *River Research and Applications* **21**: 693–717.

Owens ON, Walling DE. 2002. The phosphorus content of fluvial sediment in rural and industrialized river basins. *Water Research* **36**: 685–701.

Palmer JA, Schillling KE, Isenhart TM, Schultz RC, Tomer MD. 2014. Streambank erosion rates and loads within a single watershed: bridging the gap between temporal and spatial scales. *Geomorphology* **209**: 66–78.

Perry M, Hollis D, Elms M. 2009. *The generation of daily gridded datasets and rainfall for the UK, Climate Memorandum 24*. Met Office. National Climate Information Centre: Exeter, UK.

Prosser I, Young I, Rustomji P, Hughes A, Moran C. 2001. A model of river sediment budgets as an element of river health assessment. In *Proceedings of MODSIM 2001 - International Congress on Modelling and Simulation*, Canberra, Australia; 1–6.

Rhoades EL, O'Neal MA, Pizzuto JE. 2009. Quantifying bank erosion on the South River from 1937 to 2005, and its importance in assessing Hg contamination. *Applied Geography* **29**: 125–134.

Rowan JS, Barnes SJA, Hetherington SL, Lambers B, Parsons F. 1995. Geomorphology and pollution: the environmental impacts of lead mining, Leadhills, Scotland. *Journal of Geochemical Exploration* **52**: 57–65.

Sharpley AN, Williams JR (eds). 1990. Epic-Erosion/Productivity Impact Calculator: 1. Model Documentation. US Department of Agriculture Technology Bulletin No. 176–235.

Simon A, Collison A. 2002. Quantifying the mechanical and hydrologic effects of riparian vegetation on streambank stability. *Earth Surface Processes and Landforms* **27**: 527–546.

Simon A, Curini A, Darby SE, Langendoen EJ. 2000. Bank and near-bank processes in an incised channel. *Geomorphology* **35**: 193–217.

Soulsby C, Youngson A, Moir H, Malcolm IA. 2001. Fine sediment influence on salmonid spawning habitat in a lowland agricultural stream: a preliminary assessment. *Science of the Total Environment* **265**: 295–307.

Surian N, Mao L. 2009. Morphological effects of different channel-forming discharges in a gravel-bed river. *Earth Surface Processes and Landforms* **1107**: 1093–1107.

Thorne CR. 1982. Processes and mechanisms of river bank erosion. In *Gravel-Bed Rivers*, Hey RD, Bathurst JC, Thorne CR (eds). Wiley: Chichester.

Van Liew M, Arnold JG, Garbrecht JG. 2003. Hydrologic sumulation on agricultural watersheds: choosing between two models. *Transactions of the ASAE* **46**: 1539–1551.

Walling DE. 2005. Tracing suspended sediment sources in catchments and river systems. *Science of the Total Environment* **344**: 159–184.

Walling DE, Collins AL, Jones PA, Leeks GJL, Old G. 2006. Establishing fine-grained sediment budgets for the Pang and Lambourn LOCAR catchments, UK. *Journal of Hydrology* **330**: 126–141.

Walling DE, Collins AL, Stroud RW. 2008. Tracing suspended sediment and particulate phosphorus sources in catchments. *Journal of Hydrology* **350**: 274–289.

Wilkinson SN, Dougall C, Kinsey-Henderson AE, Searle RD, Ellis RJ, Bartley R. 2014. Development of a time-stepping sediment budget model for assessing land use impacts in large river basins. *Science of the Total Environment* **468–469**: 1210–1224.

Wilkinson SN, Prosser IP, Rustomji P, Read AM. 2009. Modelling and testing spatially distributed sediment budgets to relate erosion processes to sediment yields. *Environmental Modelling and Software* **24**: 489–501.

Winterbottom SJ, Gilvear DJ. 2000. A GIS-based approach to mapping probabilities of river bank erosion: regulated river Tummel, Scotland. *Regulated Rivers: Research and Management* **16**: 127–140.

Wösten JHM, Lilly A, Nemes A, Le Bas C. 1999. Development and use of a database of hydraulic properties of European soils. *Geoderma* **90**: 169–185.

